

# Solving Deep Reinforcement Learning Benchmarks with Linear Policy Networks

Annie Wong<sup>\*†</sup>, Jacob de Nobel<sup>\*</sup>, Thomas Bäck, Aske Plaat, Anna V. Kononova

Leiden Institute of Advanced Computer Science, Leiden University

## Abstract

Although Deep Reinforcement Learning (DRL) methods can learn effective policies for challenging problems such as Atari games and robotics tasks, algorithms are complex and training times are often long. This study investigates how evolution strategies (ES) perform compared to gradient-based deep reinforcement learning methods. We use ES to optimize the weights of a neural network via neuroevolution, performing direct policy search. We benchmark both regular networks and policy networks consisting of a single linear layer from observations to actions; for three classical ES methods and for three gradient-based methods such as PPO. Our results reveal that ES can find effective linear policies for many RL benchmark tasks, in contrast to DRL methods that can only find successful policies using much larger networks suggesting that current benchmarks are easier to solve than previously assumed. Interestingly, also for higher complexity tasks, ES achieves results comparable to gradient-based DRL algorithms. Furthermore, we find that by directly accessing the memory state of the game, ES are able to find successful policies in Atari, outperforming DQN. While gradient-based methods have dominated the field in recent years, ES offers an alternative that is easy to implement, parallelize, understand, and tune.

## 1 Introduction

Gradient-based deep reinforcement learning (DRL) has achieved remarkable success in various domains by enabling agents to learn complex behaviors in challenging environments based on their reward feedback, such as StarCraft [Vinyals *et al.*, 2019] and Go [Silver *et al.*, 2016]. However, new methods are often benchmarked on simpler control tasks from OpenAI Gym, including the locomotion tasks from MuJoCo [Haarnoja *et al.*, 2018], or Atari games

[Mnih *et al.*, 2015]. While it simplifies the comparison between different approaches, these benchmarks may lack sufficient complexity, and performance may not always transfer to more complicated tasks. Additionally, several studies have indicated that DRL results are often hard to reproduce [Islam *et al.*, 2017], attributing these difficulties to the impact of the random seeds [Henderson *et al.*, 2018] and the choice of hyperparameters [Eimer *et al.*, 2023].

Evolution Strategies (ES) [Rechenberg, 1965; Bäck *et al.*, 1991], a family of black-box optimization algorithms from the field of Evolutionary Algorithms (EAs) [Bäck *et al.*, 2023] have been studied as an alternative way to optimize neural network weights, as opposed to conventional gradient-based backpropagation [Salimans *et al.*, 2017; Such *et al.*, 2017]. An ES is used to learn a controller for an RL task by directly optimizing the neural network’s weights, which parameterize the RL policy. In this context, the ES is intrinsically an RL method that performs direct policy search, through *neuroevolution* [Igel, 2003]. In supervised learning, gradient-based methods are often much more efficient than ES for training NN weights, though more likely to be trapped in local optima [Mandischer, 2002]. For RL, the need to balance exploration with exploitation in gradient-based approaches incurs more training steps to learn an optimal policy [Igel, 2003], making ES an interesting alternative. While EAs are not necessarily more sample-efficient, ES can be more easily parallelized and scaled, offering the possibility for faster convergence in terms of wall-clock time, and, being a global search method, are less likely to get stuck in a local optimum [Morse and Stanley, 2016].

We benchmark three ES and three gradient-based RL methods on well-known RL tasks to understand the circumstances that favor ES over gradient-based methods. In particular, we study the optimization of policy networks that consist of a single linear layer, as they reduce the dimensionality of the problem [Chrabszcz *et al.*, 2018; Rajeswaran *et al.*, 2017]. We compare these results to the larger networks that are used by common gradient-based methods. Our main contributions are as follows:

- ES can find effective linear policies for many RL benchmark tasks. In contrast, methods based on gradient descent need vastly larger networks.
- Contrary to the prevailing view that ES are limited to

<sup>\*</sup>Equal contribution

<sup>†</sup>Corresponding author: Annie Wong

a.s.w.wong@liacs.leidenuniv.nl

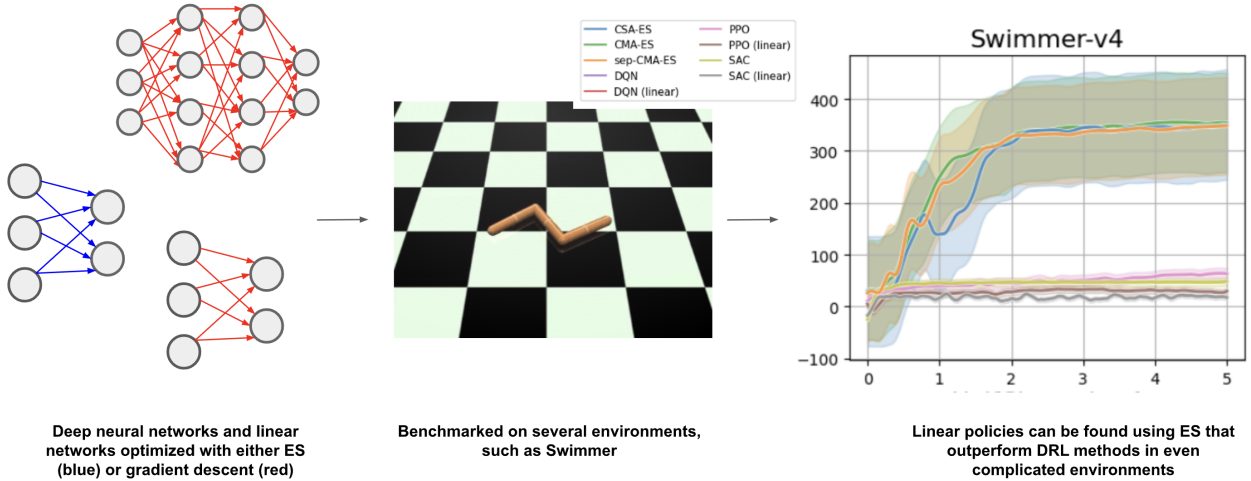


Figure 1: This study investigates how evolution strategies compare to gradient-based reinforcement learning methods in optimizing the weights of linear policies. We use both linear networks as the original DRL architectures to learn policies. We find that ES can learn linear policies for numerous tasks where DRL cannot, and in many instances, even surpasses the performance of the original DRL networks, such as in Swimmer.

simpler tasks, they can address more complex challenges in MuJoCo. Gradient-based DRL only performs superbly in the most challenging MuJoCo environments with more complex network architectures. This suggests that common RL benchmarks may be too simple or that conventional gradient-based solutions may be overly complicated.

- Complex gradient-based approaches have dominated DRL. However, ES can be equally effective, are algorithmically simpler, allow smaller network architectures, and are thus easier to implement, understand, and tune (See Figure 1).
- We find that advanced self-adaptation techniques in ES are often not required for (single-layer) neuroevolution.

The rest of the paper is organized as follows: Section 2 discusses the background and related work of ES and DRL, our algorithms are discussed in Section 3, the results are in Section 4, conclusions are in Section 5.

## 2 Background and Related Work

In RL, an agent learns from feedback through rewards and penalties from its environment [Sutton and Barto, 2018]. RL problems are formulated as a Markov Decision Process  $\langle S, A, P, R, \gamma \rangle$ , where  $S$  is the set of states in the environment,  $A$  the set of actions available to the agent,  $P$  the probability of subsequent state transitions,  $R$  the reward function, and  $\gamma \in [0, 1]$  the discount factor [Bellman, 1957]. A policy  $\pi$  can be computed of which action to take in each state. The policy in DRL is typically represented by a deep neural network to map states to actions (probabilities). RL aims to find the optimal policy  $\pi^*$  that maximizes the expected cumulative reward of a state. RL algorithms approach this goal in different ways [Plaat, 2022]. The most common techniques include value-function estimation [Watkins and Dayan, 1992;

Mnih *et al.*, 2015], policy gradient methods [Williams, 1992], actor-critic methods [Konda and Tsitsiklis, 1999; Schulman *et al.*, 2017; Haarnoja *et al.*, 2018], and learning a model of the environment [Hafner *et al.*, 2020; Plaat *et al.*, 2023].

ES are a distinct class of evolutionary algorithms that are particularly suitable for optimization problems in continuous domains. ES begin with a population of randomly initialized candidate solutions in  $\mathbb{R}^n$ , with solutions represented as  $n$ -dimensional vectors denoted by  $\mathbf{x}$  (like the policy) and a given objective function  $f : \mathbb{R}^n \rightarrow \mathbb{R}$  (like the reward). Via perturbations using a parameterized multivariate normal distribution, selection, and sometimes recombination, solutions evolve towards better regions in the search space [Bäck *et al.*, 1991]. Evolving neural networks with EAs is called neuroevolution and can include the optimization of the network's weights, topology, and hyperparameters [Stanley *et al.*, 2019]. Using ES to evolve a neural network's weights is similar to policy gradient methods in RL, where optimization applies to the policy's parameter space.

Gradient-based deep RL has successfully tackled high-dimensional problems, such as playing video games with deep neural networks encompassing millions parameters [Mnih *et al.*, 2015; Vinyals *et al.*, 2019]. However, state-of-the-art ES variants are limited to smaller numbers of parameters due to the computational complexity of, for example, the adaptation of the covariance matrix of the search distribution. Covariance Matrix Adaptation Evolution Strategy (CMA-ES) is often used for dimensionality lower than  $n \leq 100$  [Müller and Glasmachers, 2018], and problems with a dimensionality  $n \geq 10.000$  become nearly impossible due to the memory requirements [Loshchilov, 2014]. However, recent advancements have restricted the covariance matrix, in its simplest form, to its diagonal, to reduce the computational complexity [Ros and Hansen, 2008; Loshchilov, 2014; Nomura and Ono, 2022]. Others sample

from lower-dimensional subspaces [Maheswaranathan *et al.*, 2019; Choromanski *et al.*, 2019].

In 2015, DRL reached a milestone by achieving superhuman performance in Atari games using raw pixel input [Mnih *et al.*, 2015]. This breakthrough marked a shift in RL towards more complicated, high-dimensional problems and a shift from tabular to deep, gradient-based methods. For simpler tasks, the CMA-ES has been used to evolve neural networks for pole-balancing tasks, benefiting from covariance matrix to find parameter dependencies, enabling faster optimization [Igel, 2003; Heidrich-Meisner and Igel, 2009]. While the use of evolutionary methods for RL can be traced back to the early 90s [Whitley *et al.*, 1993; Moriarty and Mikkulainen, 1996], the paper by [Salimans *et al.*, 2017] rekindled interest in ES from the field of RL as an alternative for gradient-based methods in more complicated tasks. Researchers showed that a natural evolution strategy (NES) can compete with deep RL in robot control in MuJoCo and Atari games due to its ability to scale over parallel workers. In contrast to deep methods where entire gradients are typically shared, the workers only communicate the fitness score and the random seed to generate the stochastic perturbations of the policy parameters. Studies have subsequently demonstrated that simpler methodologies can yield results comparable to NES, such as a classical ES [Chrabaszcz *et al.*, 2018] and Augmented Random Search [Mania *et al.*, 2018], which closely resembles a global search heuristic from the 1990s [Salomon, 1998]. In addition, when separating the computer vision task from the actual policy in playing Atari, the size of the neural network can be drastically decreased [Cuccu *et al.*, 2018], and policies with a single linear layer, mapping states directly to actions, can effectively solve the continuous control tasks [Chrabaszcz *et al.*, 2018; Rajeswaran *et al.*, 2017]. The development of dimension-lowering techniques, such as world models [Ha and Schmidhuber, 2018; Hafner *et al.*, 2020] and autoencoders [Hinton and Salakhutdinov, 2006], also opens up new possibilities for ES to effectively solve more complex problems by simplifying them into more manageable forms.

### 3 Methods

We implement three ES methods and benchmark them against three popular gradient-based DRL methods.

#### 3.1 Gradient-Based Algorithms

We use three popular gradient-based DRL algorithms: Deep Q-learning [Mnih *et al.*, 2015], Proximal Policy Optimization [Schulman *et al.*, 2017], and Soft Actor-Critic [Haarnoja *et al.*, 2018]. We summarize the main gradient-update ideas below.

##### Deep Q-Learning

Deep Q-learning (DQN) combines a deep neural network with Q-learning to learn the value function in a high-dimensional environment [Mnih *et al.*, 2015]. Each experience tuple  $(s_t, a_t, r_t, s_{t+1})$  is stored in a replay buffer. The agent randomly selects a batch of experiences to update the value function. The replay buffer breaks the correlation between consecutive experiences, leading to lower variance.

The primary Q-network weights  $\theta$  are updated every training step by minimizing the expectation of the squared difference between the predicted Q-value of the current state-action pair  $Q(s, a; \theta)$  and the target Q-value  $Q(s', a'; \theta^-)$ :

$$L(\theta) = \mathbb{E} \left[ \left( r + \gamma \max_{a'} Q(s', a'; \theta^-) - Q(s, a; \theta) \right)^2 \right]$$

The weights from the primary Q-network are copied every  $N$  timesteps to a separate target network  $\theta^- \leftarrow \theta$  to prevent large oscillations in the loss function's target values.

#### Proximal Policy Optimization

Proximal Policy Optimization (PPO) was introduced to improve the complexity of earlier policy gradient methods [Schulman *et al.*, 2017]. PPO introduces a simpler, clipped objective function:

$$L^{CLIP}(\theta) = \hat{\mathbb{E}}_t \left[ \min(r_t(\theta) \hat{A}_t, \text{clip}(r_t(\theta), 1 - \epsilon, 1 + \epsilon) \hat{A}_t) \right]$$

where  $\hat{\mathbb{E}}_t$  denotes the empirical expectation over a finite batch of samples, the probability ratio  $r_t(\theta)$  reflects the probability of an action under the current policy compared to the previous policy,  $\hat{A}_t$  is the advantage estimate at timestep  $t$ , and  $\epsilon$  is a hyperparameter defining the clipping range. The clipping mechanism clips the ratio  $r_t(\theta)$  within the range  $[1 - \epsilon, 1 + \epsilon]$ .

#### Soft Actor-Critic

SAC objective's function maximizes the expected return and entropy simultaneously to ensure a balanced trade-off between exploitation and exploration:

$$\pi^* = \arg \max_{\pi} \sum_t \mathbb{E}_{(s_t, a_t) \sim \rho_{\pi}} [r(s_t, a_t) + \alpha H(\pi(\cdot | s_t))],$$

where  $\alpha$  is the temperature parameter that scales the importance of the entropy  $H(\pi(\cdot | s_t))$  of the policy  $\pi$  given the state  $s_t$ . SAC updates its Q-value estimates using a soft Bellman backup operation that includes an entropy term:

$$Q_{\text{new}}(s_t, a_t) = \mathbb{E}_{s_{t+1} \sim \mathcal{E}} [r(s_t, a_t) + \gamma (Q_{\text{old}}(s_{t+1}, a_{t+1}) - \alpha \log \pi(a_{t+1} | s_{t+1}))].$$

SAC employs twin Q-networks to mitigate overestimation bias and stabilize policy updates by using the minimum of their Q-value estimates.

#### 3.2 Evolution Strategies

ES are designed for solving continuous optimization problems  $\text{maximize}_{\mathbf{x}} f(\mathbf{x})$ , where  $f : \mathbb{R}^n \rightarrow \mathbb{R}$ . The ES methods are used here to optimize the neural network parameters for the policy function, i.e., the ES is used for neuroevolution of the weights of the neural network that represents the policy. The methods are variants of derandomized ES and use a parameterized normal distribution  $\mathcal{N}(\mathbf{m}^{(g)}, \sigma^{(g)} \mathbf{C}^{(g)})$  to control the direction of the search. The algorithm adapts the parameters of the search distribution to achieve fast convergence (Algorithm 1).

The ES samples  $\lambda$  offspring from its mutation distribution at each iteration. By selecting the  $\mu \leq \lambda$  most promising offspring to update its parameters, it moves to regions of higher

---

**Algorithm 1** Generic ES

---

**Require:** Objective function  $f$ , number of offspring  $\lambda$ , number of parents  $\mu$ , initial estimates for  $\mathbf{m}^{(0)}$  and  $\sigma^{(0)}$   
 $\mathbf{C}^{(0)} \leftarrow \mathbf{I}_n$   
**for**  $g$  in  $1, 2, \dots$  **do**  
    Sample  $\lambda$  candidates  $\mathbf{x}_i \sim \mathcal{N}(\mathbf{m}^{(g)}, \sigma^{(g)} \mathbf{C}^{(g)})$   
    Evaluate objective function  $f_i \leftarrow f(\mathbf{x}_i)$   
    Select and rank  $\mu$  best candidates  
    Adapt  $\mathbf{m}^{(g+1)}, \sigma^{(g+1)}, \mathbf{C}^{(g+1)}$   
**end for**

---

optimality. After sorting the  $\mu$  offspring by fitness ranking, the mean of the search distribution is updated via weighted recombination:

$$\mathbf{m}^{(g+1)} = \mathbf{m}^{(g)} + c_m \sum_{i=1}^{\mu} w_i (\mathbf{x}_i - \mathbf{m}^{(g)})$$

The ES variants adapt, with increasing complexity, the scale  $\sigma^{(g)}$  and shape  $\mathbf{C}^{(g)}$  of the mutation distribution. The Cumulative Step-size Adaptation Evolution Strategy (CSA-ES) only adapts  $\sigma^{(g)}$ , producing exclusively isotropic (i.e.  $\mathbf{C}^{(g)} = \mathbf{I}_n$ ) mutations during optimization. The separable Covariance Matrix Adaptation Evolution Strategy (sep-CMA-ES) additionally adapts the diagonal entries of the covariance matrix  $\mathbf{C}^{(g)}$ , producing mutation steps with arbitrary scaling parallel to each coordinate axis. Finally, the CMA-ES adapts the full covariance matrix, which allows the mutation distribution to scale to arbitrary rotations. Figure 2 illustrates the evolution of the mutation distribution for each of these three methods when optimizing a two-dimensional quadratic function. The figure shows that the mutation distribution guides the search, favoring selected mutation steps with high probability [Hansen and Ostermeier, 2001]. The CSA-ES uses a process called cumulation of historically selected mutation steps in order to update the value of the global step size parameter  $\sigma^{(g)}$ . We implemented the algorithm following [Chotard *et al.*, 2012], using recommended hyperparameter settings. While several modifications of the CMA-ES have been developed over the years, we implemented a canonical version of the algorithm, as first introduced in [Hansen and Ostermeier, 2001]. The update of the full covariance matrix becomes computationally impractical for  $n > 100$ , but the sep-CMA-ES, which we implemented according to [Ros and Hansen, 2008], does not suffer from this restriction. As shown in Figure 2, this algorithm only computes variances for each coordinate axis, which makes it applicable to much higher dimensions, as the computational complexity for the update of the mutation distribution scales only linearly with  $n$ .

### 3.3 Network Architecture

We compare the performance of linear policies trained through neuroevolution by ES with gradient-based methods inspired by earlier studies demonstrating this approach's feasibility [Mania *et al.*, 2018; Rajeswaran *et al.*, 2017]. For the ES, only linear policies are trained, defined as a linear mapping from states to actions, activated by either an argmax

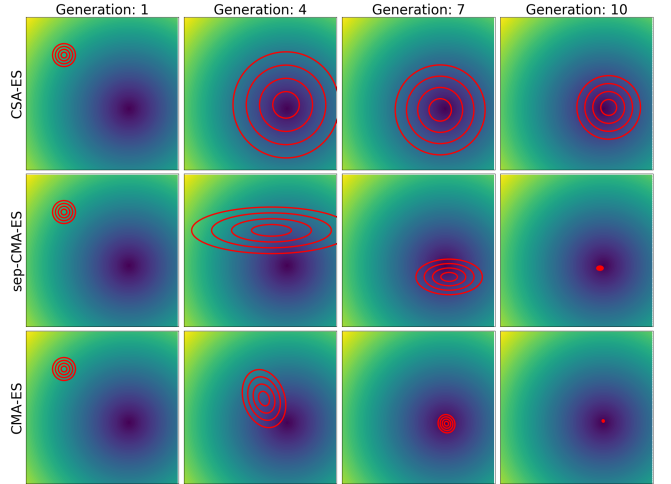


Figure 2: Adaptation of the mutation distribution for three different Evolution Strategies for the first ten generations of a two-dimensional quadratic function. Function values are shown with color; darker indicates lower (better). Top row: mutation distribution for CSA-ES; middle row: sep-CMA-ES; bottom row: CMA-ES

or  $\tanh$  function for discrete and continuous action spaces, respectively (no hidden layer: a fully connected shallow network). We use the gradient-based methods to train the same linear policies for each control task. Table 2 (Supplementary material) shows the number of trainable weights for each environment for a linear policy. Additionally, a network architecture based on the original studies for each of the gradient-based methods is trained for comparison. We employ the architecture from the original studies for PPO [Schulman *et al.*, 2017] and SAC [Haarnoja *et al.*, 2018]. For DQN, we use the default architecture from CleanRL's library, which has been tested across multiple control environments and showed good results [Huang *et al.*, 2022]. Specifics for these architectures and other hyperparameters can be found in the supplementary material. We do not train these deep architectures using ES, as they only serve as a benchmark to demonstrate the intended usage of the gradient-based algorithms, and self-adaptation mechanisms are increasingly less useful for such high dimensions [Chrabaszcz *et al.*, 2018].

### 3.4 Experimental Setup

We conduct experiments on common control tasks of varying complexity levels from the Gymnasium API [Towers *et al.*, 2023]. For each of the considered environments, five runs using different random seeds are conducted for each algorithm/control task combination to test the stability of each approach. Value-based DQN is only used for environments with discrete action spaces, SAC for continuous action spaces, and PPO and ES are used for both action spaces. The RL algorithms are implemented using the cleanRL library<sup>1</sup> that has been benchmarked across several environments; we removed the hidden layers for the linear network. The specifics of the Evolution Strategies (ES) implementations are detailed in

<sup>1</sup><https://github.com/vwxyzjn/cleanrl/tree/master>

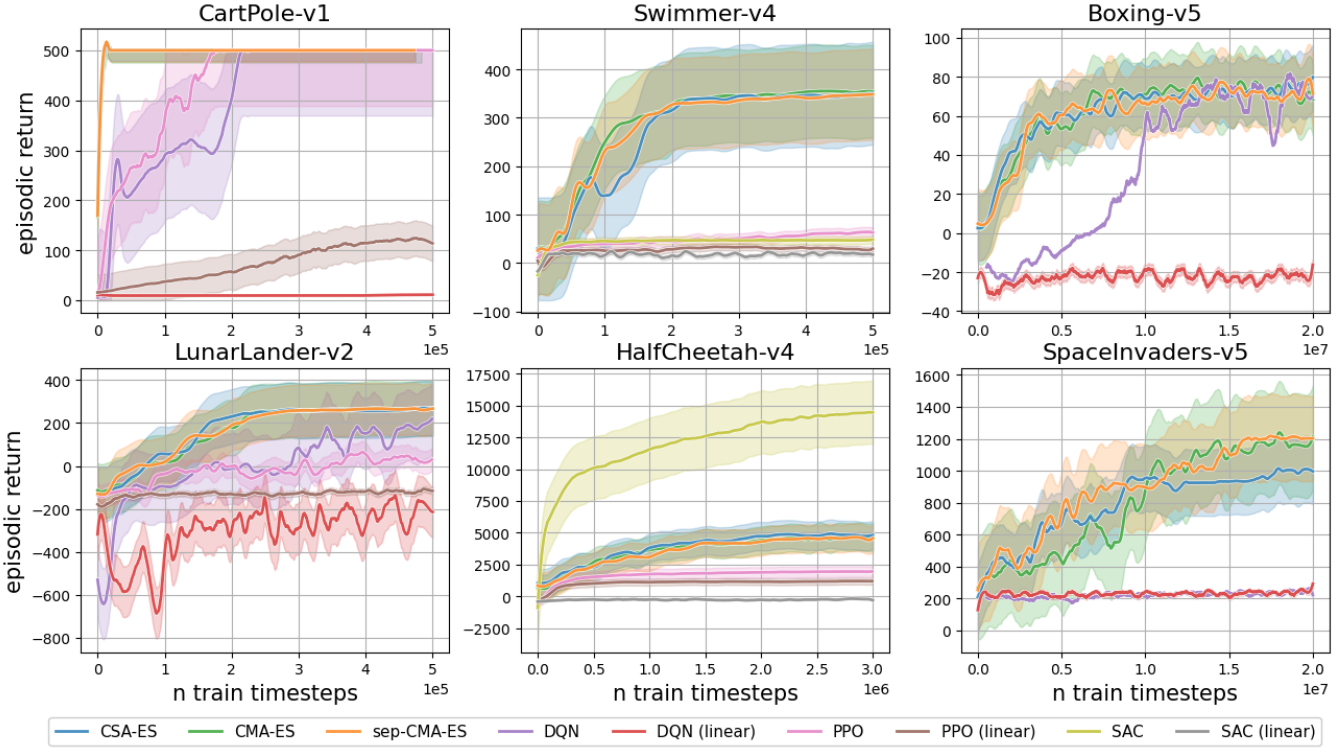


Figure 3: Training curves for the CartPole, LunarLander, Swimmer, HalfCheetah, Boxing, and SpaceInvaders environments. Episodic return (calculated using 5 test episodes) vs. the number of training timesteps is shown. Each curve represents the median of 5 trial runs conducted with different random seeds; the shaded area denotes standard deviations. The results show that ES solve the classic control environments Cartpole and LunarLander almost immediately, surpassing the gradient descent methods. Even for the more difficult Swimmer environment, ES find a linear policy outperforming DRL in terms of timesteps and performance. While SAC outperforms all other methods in Cheetah, linear ES outperforms classic PPO. For the Atari environments, Boxing and Space Invaders, ES is able to learn a linear policy from the RAM input, while linear DQN fails to do so, and only for Boxing deep DQN finds a successful policy.

Algorithm	CSA-ES	CMA-ES	sep-CMA	Random	Human	DQN	ES*
Atlantis	84690	87100	<b>88580</b>	12850	29028	85641	103500
B. Rider	2215	1967	2222	363.9	5775	<b>6846</b>	5072
Boxing	96.0	<b>96.8</b>	95.1	0.1	4.3	71.8	100
C. Climber	36170	29290	32940	10781	35411	<b>114103</b>	57600
Enduro	65.1	58.9	69.0	0	<b>309.6</b>	301.8	102
Pong	5.7	7.4	7.1	-20.7	9.3	<b>18.9</b>	21
Q*Bert	7355	5732	7385	163.9	<b>13455</b>	10596	14700
Seaquest	959	948	954	68.4	<b>20182</b>	5286	1470
S. Invaders	1640	1972	1488	148	1652	<b>1976</b>	2635

Table 1: Average maximum score per game across trials. The rightmost column shows the best-performing ES episode per game. For comparison, the scores for DQN, a random agent, and a Human player taken from [Mnih *et al.*, 2015] are shown. The highest scores are shown in boldface. The results show that an ES outperforms the original DQN scores for Atlantis and Boxing. For the other games, the highest score is attained by the DQN agent, although CMA-ES achieves a score almost identical to DQN on SpaceInvaders. Furthermore, the best ES policy often matches the performance of DQN, demonstrating that a linear policy can be just as effective. Standard deviation values are provided in Table 1 in the supplementary material.

the repository, the link to which is provided in the footnote<sup>2</sup>. Since the environments are stochastic, we report the median episodic return, calculated over five test episodes. As was discussed in [Salimans *et al.*, 2017], for ES, the wall-clock time required to solve a given control task decreases linearly with

the number of parallel workers available. This allows us to do many more evaluations of the environment than is feasible with gradient-based RL. For fairness of comparison, we limit the difference in the number of training time steps allowed by a single order of magnitude. Specific hyper-parameters used for each environment can be found in the supplementary

<sup>2</sup>anonymized for reviewing

material, including hardware. For the ES, we initialize each experiment with  $\mathbf{m}^{(0)} = \mathbf{0}$ . We calculate a rolling mean and variance of the observations of the environment during each run. These values are then used to normalize each state observation to standard normal entries by subtracting this rolling mean and dividing by the standard deviation.

### Classic RL Environments

The first set of experiments includes the classic control tasks Cartpole, Acrobot, and Pendulum. We include BipedalWalker and LunarLander from the Box2D simulations for slightly more complex dynamics. Each run uses a maximum of 500 000 timesteps for each environment. The exception to this is the BipedalWalker task, for which  $2 \cdot 10^6$  timesteps are used.

### MuJoCo Simulated Robotics

We evaluate the algorithms on the MuJoCo environments [Todorov *et al.*, 2012] for higher complexity levels, including Hopper, Walker2D, HalfCheetah, Ant, Swimmer, and Humanoid. Table 3 (Supplementary material) provides training details. As was noted by [Mania *et al.*, 2018], ES methods have exploration at the policy level, whereas gradient-based methods explore on the action level. In the locomotion tasks, a positive reward is provided for each time step where the agent does not fall over. This causes the ES method to stay in a local optimum when the agent stays upright but does not move forward (the gradient-based methods do not get stuck). Following [Mania *et al.*, 2018], we modified the reward function for these environments for ES, subtracting the positive stability bonus and only rewarding forward locomotion.

### Atari Learning Environment

Finally, we benchmark DQN against the ES with linear policies on games from the Atari suite. To demonstrate the effectiveness of linear policies for these high-dimensional tasks, we take inspiration from the approach by [Cuccu *et al.*, 2018] and separate the computer vision task from the control task. We train the ES agents on the 128 bytes of the Random Access Memory (RAM) in the simulated Atari console. This drastically reduces the input dimensionality of the controller, allowing for the training of smaller policies. This assumes that the random access memory sufficiently encodes the state of each game without having to extract the state from the raw pixel images. It should be noted that not for all games is RAM information sufficient to train a controller and that for some games, DQN is easier to train on pixel images than on RAM input [Sygnowski and Michalewski, 2017]. Since we evaluate linear policies, we fix frame skipping to 4, with no sticky actions [Machado *et al.*, 2018], similar to the settings used in [Mnih *et al.*, 2015]. For each run, the ES were trained for 20 000 episodes, where the maximum episode length was capped at 270 000 timesteps. The gradient-based methods were trained for a maximum of  $2 \cdot 10^7$  timesteps.

## 4 Results

In this section, we present the results of our experiments (more details, including training curves and tables with summary statistics, can be found in the Supplementary material). Here, we focus on a selection of environments (Figure 3).

### 4.1 Classics RL Environments

The first column of Figure 3 shows the training curves for the gradient-based methods and for ES on the CartPole and LunarLander environments (the Supplementary material has more). For both environments, the ES policies outperform the deep gradient-based methods with just a simple linear policy. For CartPole, the results are even more surprising, as the ES policies are able to solve the environment in the first few iterations of training through pure random sampling from a standard normal distribution. The deep gradient-based methods, on the other hand, require around  $2 \cdot 10^5$  timesteps in order to solve CartPole. The gradient-based methods are unable to find a good linear policy for CartPole. This pattern persists for LunarLander, where, even though the ES requires around  $2 \cdot 10^5$  timesteps to solve the environment, the gradient-based methods cannot find a good linear policy at all. While the deep gradient-based methods eventually seem to catch up to the ES, it still requires more than  $5 \cdot 10^5$  timesteps to train a stable policy for LunarLander. For the BipedalWalker task (see Supplementary material), DQN and PPO are able to find good policies, with the gradient-based methods requiring fewer timesteps. Only SAC is able to solve Pendulum within  $5 \cdot 10^5$  timesteps. For Acrobot, again, the ES are able to solve the environment almost instantly, while the gradient-based methods require a good number of environment interactions to do so.

### 4.2 MuJoCo Simulated Robotics

The center column of Figure 3 shows that the ES policies are much better at finding a policy for the Swimmer environment, while for HalfCheetah, SAC greatly outperforms all other methods. However, ES outperforms PPO. Moreover, none of the gradient-based methods are able to find a good linear policy for HalfCheetah and Swimmer. This pattern holds for almost all MuJoCo experiments; only for the Ant environment can PPO find a linear policy with decent performance. Overall, as the number of weights increases, the performance of the ES lags behind the deep gradient-based methods (see Table 2 in the Supplementary material). Nevertheless, even though ES generally require more timesteps, they can still find good linear policies for most environments, which are just as effective as policies found by vastly larger networks (see Table 4 in the Supplementary material). Even for the most complex of these environments, Humanoid, the ES are able, in several trials, to find a linear policy that has a higher episodic return,  $\approx 8000$  (averaged over 5 test episodes with different random seeds), than was found by the best deep gradient-based method, SAC. Furthermore, ES timesteps are quicker and easier to parallelize, meaning experiments are much faster to run.

### 4.3 Atari Learning Environment

The last column of Figure 3 shows the training curves of ES vs. DQN for the Atari games SpaceInvaders and Boxing. The figure shows that when training agents that use the controller’s RAM state as observations, ES outperform linear DQN in most cases. CrazyClimber (Supplementary material) is the only exception, for which the performance of ES and linear DQN is similar. Even comparing against deep DQN

trained on RAM memory, we find that for both the games in Figure 3, the ES yield better policies and require fewer environment interactions. In addition, Table 1 shows the average highest score per trial for each of the tested games for the ES, compared against the numerical results presented in [Mnih *et al.*, 2015] for a Human, Random and a DQN player that uses pixel input. The table additionally shows the highest score attained by any ES in any trial, averaged over 5 test episodes. For both Atlantis and Boxing, an ES achieves the highest score. For all the other games tested, the DQN agent earned a higher score than all RAM-trained ES, although CMA-ES achieved a score almost identical to DQN on SpaceInvaders. This score is attained by an agent that uses a linear policy consisting of only 768 weights, while the policy trained by DQN has  $\approx 1.5 \cdot 10^6$  (pixel-based, deep policy network). Moreover, the best-found policy by any ES is often competitive with DQN. This indicates that a linear policy, which is competitive with pixel-based DQN, does exist.

## 5 Discussion and Conclusion

In this study, we have studied different ways to optimize reinforcement learning policies with conventional deep learning gradient-based backpropagation methods as used in DQN, PPO, and SAC, and with three evolution strategy methods (ES). We have applied these methods to several classic reinforcement learning benchmarks. For these methods, we trained the regular deep network as conventionally used, as well as a neural network with no hidden layers, i.e., a linear mapping from states to actions, as a low-complexity controller for each environment. In many of the tested environments, the linear policies trained with the ES are on par or, in some cases, even better controllers than the deep policy networks trained with the gradient-based methods. Additionally, the gradient-based methods are often ineffective at training these simple policies, requiring much deeper networks. For our experiments on Atari, we find that by accessing the RAM memory of the Atari controller, ES methods can find a linear policy that is competitive with "superhuman" DQN [Mnih *et al.*, 2015]. It should be noted that there are certain high-complexity environments where the deep gradient-based methods yield better policies, e.g. SAC for HalfCheetah. However, even for these environments, linear policies exist that are competitive and much more easily interpretable.

We conclude that conventional gradient-based methods might be overly complicated or that more complex benchmarks are required to properly evaluate algorithms. In fact, even for the most complex locomotion task included in our experiments, the Humanoid environment, the CMA-ES was able to find a linear policy that was competitive with state-of-the-art methods. As the ES are stochastic algorithms, they were not able to find these policies for every trial run, but our results show that such policies do exist. We expect the search landscapes for these environments to be deceptive and multimodal, and future work could help discover effective algorithms for more consistently training these linear policy networks, for example, using niching methods [Shir and Bäck, 2005]. We hypothesize that gradient-based methods may struggle to find linear policies due to the multimodal nature

of the search landscape, a phenomenon also seen in supervised learning [Kawaguchi, 2016]. Counterintuitively, with gradient-based methods, it seems more straightforward to train deeper architectures than shallower ones with far fewer weights, as was also shown by [Schwarzer *et al.*, 2023]. We note that gradient-based methods are essentially local search methods, requiring heuristically controlled exploration, while ES, in the early phases of optimization, are performing global search, producing more diverse solutions. This also becomes evident in the more simple environments, such as CartPole, where the ES are able to almost instantly sample the optimal policy, while the gradient-based methods have a much harder time.

Moreover, we find many counterexamples to the prevailing view that ES are less sample efficient than the gradient-based methods. For many of the low to medium-complexity environments, the ES are actually more sample efficient and require fewer environment interactions than the deep gradient-based methods. On the other hand, for the more complex environments, and with increasing dimensionality, we find that the ES can take more time steps to converge than the deep gradient-based methods. This is to be expected, as the self-adaptation mechanisms that are central to the ES become increasingly ineffective for larger dimensions [Chrabszcz *et al.*, 2018; Müller and Glasmachers, 2018]. We have compared three ES, that, with increasing levels of complexity, adapt the shape of the mutation distribution in order to converge the search. Our results indicate that updates of the covariance matrix are often not required and that performing step size adaptation is sufficient. While we expect the search landscape to be multimodal, relative scaling and rotation of search coordinates seem absent, allowing isotropic mutations to be effective for these problems. This would also explain the effectiveness of the approach demonstrated in [Maheswaranathan *et al.*, 2019], which would be heavily impacted by conditioning on the search space. However, this may be explained because optimizing a single linear layer may exhibit less inherent variance and covariance than multiple layers.

Overall, we have demonstrated the potential of linear policies on popular RL benchmarks. We showed that ES are effective optimizers for these policies compared to gradient-based methods. Additionally, we note that ES are simpler in design, have fewer hyperparameters, and are trivially parallelizable. Hence, ES can perform more environment interactions within the same time frame [Salimans *et al.*, 2017]. Moreover, evaluating linear policies is faster than evaluating one or sometimes several deep architectures, making the training much more expedient regarding wall-clock time. As the need for energy-efficient policy networks increases, our results warrant a closer look at ES for RL and training of simpler policies for tasks currently considered complex. For future work, we aim to extend our benchmark with more types of classical ES and strategies for multimodal optimization [Preuss, 2015]. Additionally, it would be interesting to study the effect of the step-size adaptation methods in the presence of one or more hidden layers. Next, we will explore the potential of linear networks for other applications. Inspired by works such as [Cuccu *et al.*, 2018], we will look at more com-

plex Atari games to see if they can also be solved by simple, energy-efficient means.

## References

[Bäck *et al.*, 1991] T Bäck, F Hoffmeister, and H-P Schwefel. A survey of evolution strategies. In *Proceedings of the fourth international conference on genetic algorithms*. Citeseer, 1991.

[Bäck *et al.*, 2023] T Bäck, A V Kononova, B van Stein, H Wang, K Antonov, R Kalkreuth, J de Nobel, D Vermetten, R de Winter, and F Ye. Evolutionary algorithms for parameter optimization—thirty years later. *Evolutionary Computation*, 31(2):81–122, 2023.

[Bellman, 1957] R Bellman. A markovian decision process. *Journal of Mathematics and Mechanics*, pages 679–684, 1957.

[Choromanski *et al.*, 2019] K M Choromanski, A Pacchiano, J Parker-Holder, Y Tang, and V Sindhwani. From complexity to simplicity: Adaptive es-active subspaces for blackbox optimization. *Advances in Neural Information Processing Systems*, 32, 2019.

[Chotard *et al.*, 2012] A Chotard, A Auger, and N Hansen. Cumulative step-size adaptation on linear functions. In *Parallel Problem Solving from Nature-PPSN XII: 12th International Conference, Taormina, Italy, September 1–5, 2012, Proceedings, Part I 12*, pages 72–81. Springer, 2012.

[Chrabszcz *et al.*, 2018] P Chrabszcz, I Loshchilov, and F Hutter. Back to basics: Benchmarking canonical evolution strategies for playing atari. In *Proceedings of the Twenty-Seventh International Joint Conference on Artificial Intelligence, IJCAI-18*, pages 1419–1426. International Joint Conferences on Artificial Intelligence Organization, 2018.

[Cuccu *et al.*, 2018] G Cuccu, J Togelius, and P Cudré-Mauroux. Playing atari with six neurons. *arXiv preprint arXiv:1806.01363*, 2018.

[Eimer *et al.*, 2023] T Eimer, M Lindauer, and R Raileanu. Hyperparameters in reinforcement learning and how to tune them. In *International conference on machine learning*, 2023.

[Ha and Schmidhuber, 2018] D Ha and J Schmidhuber. World models. *arXiv preprint arXiv:1803.10122*, 2018.

[Haarnoja *et al.*, 2018] T Haarnoja, A Zhou, K Hartikainen, G Tucker, S Ha, J Tan, V Kumar, H Zhu, A Gupta, P Abbeel, et al. Soft actor-critic algorithms and applications. *arXiv preprint arXiv:1812.05905*, 2018.

[Hafner *et al.*, 2020] D Hafner, T Lillicrap, J Ba, and M Norouzi. Dream to control: Learning behaviors by latent imagination. In *International Conference on Learning Representations*, 2020.

[Hansen and Ostermeier, 2001] N Hansen and A Ostermeier. Completely derandomized self-adaptation in evolution strategies. *Evolutionary computation*, 9(2):159–195, 2001.

[Heidrich-Meisner and Igel, 2009] V Heidrich-Meisner and C Igel. Neuroevolution strategies for episodic reinforcement learning. *Journal of Algorithms*, 64(4):152–168, 2009.

[Henderson *et al.*, 2018] P Henderson, R Islam, P Bachman, J Pineau, D Precup, and D Meger. Deep reinforcement learning that matters. In *Proceedings of the AAAI conference on artificial intelligence*, volume 32, 2018.

[Hinton and Salakhutdinov, 2006] G Hinton and R Salakhutdinov. Reducing the dimensionality of data with neural networks. *science*, 313(5786):504–507, 2006.

[Huang *et al.*, 2022] S Huang, R Fernand, J Dossa, C Ye, J Braga, P Chakraborty, K Mehta, and J Araújo. Cleanrl: High-quality single-file implementations of deep reinforcement learning algorithms. *Journal of Machine Learning Research*, 23(274):1–18, 2022.

[Igel, 2003] C Igel. Neuroevolution for reinforcement learning using evolution strategies. In *The 2003 Congress on Evolutionary Computation, 2003. CEC'03.*, volume 4, pages 2588–2595. IEEE, 2003.

[Islam *et al.*, 2017] R Islam, P Henderson, M Gomrokchi, and D Precup. Reproducibility of benchmarked deep reinforcement learning tasks for continuous control. In *Reproducibility in Machine Learning Workshop (ICML)*, 2017.

[Kawaguchi, 2016] K Kawaguchi. Deep learning without poor local minima. In D. Lee, M. Sugiyama, U. Luxburg, I. Guyon, and R. Garnett, editors, *Advances in Neural Information Processing Systems*, volume 29. Curran Associates, Inc., 2016.

[Konda and Tsitsiklis, 1999] V Konda and J Tsitsiklis. Actor-critic algorithms. *Advances in neural information processing systems*, 12, 1999.

[Loshchilov, 2014] I Loshchilov. A computationally efficient limited memory cma-es for large scale optimization. In *Proceedings of the 2014 Annual Conference on Genetic and Evolutionary Computation*, pages 397–404, 2014.

[Machado *et al.*, 2018] M Machado, M Bellemare, E Tsvyattsev, J Veness, M Hausknecht, and M Bowling. Revisiting the arcade learning environment: Evaluation protocols and open problems for general agents. *Journal of Artificial Intelligence Research*, 61:523–562, 2018.

[Maheswaranathan *et al.*, 2019] N Maheswaranathan, L Metz, G Tucker, D Choi, and J Sohl-Dickstein. Guided evolutionary strategies: Augmenting random search with surrogate gradients. In *International Conference on Machine Learning*, pages 4264–4273. PMLR, 2019.

[Mandischer, 2002] M Mandischer. A comparison of evolution strategies and backpropagation for neural network training. *Neurocomputing*, 42(1):87–117, 2002.

[Mania *et al.*, 2018] H Mania, A Guy, and B Recht. Simple random search provides a competitive approach to reinforcement learning. *arXiv preprint arXiv:1803.07055*, 2018.

[Mnih *et al.*, 2015] V Mnih, K Kavukcuoglu, D Silver, A A Rusu, J Veness, M G Bellemare, A Graves, M Riedmiller, A K Fidjeland, G Ostrovski, et al. Human-level control through deep reinforcement learning. *Nature*, 518(7540):529–533, 2015.

[Moriarty and Mikkulainen, 1996] D Moriarty and R Mikkulainen. Efficient reinforcement learning through symbiotic evolution. *Machine learning*, 22:11–32, 1996.

[Morse and Stanley, 2016] G Morse and K Stanley. Simple evolutionary optimization can rival stochastic gradient descent in neural networks. In *Proceedings of the Genetic and Evolutionary Computation Conference 2016*, pages 477–484, 2016.

[Müller and Glasmachers, 2018] N Müller and T Glasmachers. Challenges in high-dimensional reinforcement learning with evolution strategies. In *Parallel Problem Solving from Nature–PPSN XV: 15th International Conference, Coimbra, Portugal, September 8–12, 2018, Proceedings, Part II 15*, pages 411–423. Springer, 2018.

[Nomura and Ono, 2022] M Nomura and I Ono. Fast moving natural evolution strategy for high-dimensional problems. In *2022 IEEE Congress on Evolutionary Computation (CEC)*, pages 1–8. IEEE, 2022.

[Plaat *et al.*, 2023] A Plaat, W Kosters, and M Preuss. High-accuracy model-based reinforcement learning, a survey. *Artificial Intelligence Review*, pages 1–33, 2023.

[Plaat, 2022] A Plaat. *Deep Reinforcement Learning*. Springer Verlag, Singapore, 2022.

[Preuss, 2015] M Preuss. *Multimodal Optimization by Means of Evolutionary Algorithms*. Springer Publishing Company, Incorporated, 1st edition, 2015.

[Rajeswaran *et al.*, 2017] A Rajeswaran, K Lowrey, E Todorov, and S Kakade. Towards generalization and simplicity in continuous control. *Advances in Neural Information Processing Systems*, 30, 2017.

[Rechenberg, 1965] I Rechenberg. Cybernetic solution path of an experimental problem. *Royal Aircraft Establishment Library Translation 1122*, 1122, 1965.

[Ros and Hansen, 2008] R Ros and N Hansen. A simple modification in cma-es achieving linear time and space complexity. In *International conference on parallel problem solving from nature*, pages 296–305. Springer, 2008.

[Salimans *et al.*, 2017] T Salimans, J Ho, X Chen, S Sidor, and I Sutskever. Evolution strategies as a scalable alternative to reinforcement learning. *arXiv preprint arXiv:1703.03864*, 2017.

[Salomon, 1998] R Salomon. Evolutionary algorithms and gradient search: similarities and differences. *IEEE Transactions on Evolutionary Computation*, 2(2):45–55, 1998.

[Schulman *et al.*, 2017] J Schulman, F Wolski, P Dhariwal, A Radford, and O Klimov. Proximal policy optimization algorithms. *arXiv preprint arXiv:1707.06347*, 2017.

[Schwarzer *et al.*, 2023] M Schwarzer, J Ceron, A Courville, M Bellemare, R Agarwal, and P Castro. Bigger, better, faster: Human-level atari with human-level efficiency. In *International Conference on Machine Learning*, pages 30365–30380. PMLR, 2023.

[Shir and Bäck, 2005] O Shir and T Bäck. Niching in evolution strategies. In *Proceedings of the 7th annual conference on Genetic and evolutionary computation*, pages 915–916, 2005.

[Silver *et al.*, 2016] D Silver, A Huang, C J Maddison, A Guez, L Sifre, G Van Den Driessche, J Schrittwieser, I Antonoglou, V Panneershelvam, M Lanctot, et al. Mastering the game of go with deep neural networks and tree search. *Nature*, 529(7587):484–489, 2016.

[Stanley *et al.*, 2019] K O Stanley, J Clune, J Lehman, and R Miikkulainen. Designing neural networks through neuroevolution. *Nature Machine Intelligence*, 1(1):24–35, 2019.

[Such *et al.*, 2017] F P Such, V Madhavan, E Conti, J Lehman, K O Stanley, and J Clune. Deep neuroevolution: Genetic algorithms are a competitive alternative for training deep neural networks for reinforcement learning. *arXiv preprint arXiv:1712.06567*, 2017.

[Sutton and Barto, 2018] R S Sutton and A G Barto. *Reinforcement learning: An introduction*. MIT press, 2018.

[Sygnowski and Michalewski, 2017] J Sygnowski and H Michalewski. Learning from the memory of atari 2600. In *Computer Games: 5th Workshop on Computer Games, CGW 2016, and 5th Workshop on General Intelligence in Game-Playing Agents, GIGA 2016, Held in Conjunction with the 25th International Conference on Artificial Intelligence, IJCAI 2016, New York, USA, July 9–10, 2016, Revised Selected Papers 5*, pages 71–85. Springer, 2017.

[Todorov *et al.*, 2012] E Todorov, T Erez, and Y Tassa. Mujoco: A physics engine for model-based control. In *2012 IEEE/RSJ international conference on intelligent robots and systems*, pages 5026–5033. IEEE, 2012.

[Towers *et al.*, 2023] M Towers, J Terry, A Kwiatkowski, J Balis, G de Cola, T Deleu, M Goulão, A Kallinteris, A KG, M Krimmel, R Perez-Vicente, A Pierré, S Schulhoff, J J Tai, A T J Shen, and O Younis. Gymnasium, March 2023.

[Vinyals *et al.*, 2019] O Vinyals, I Babuschkin, W M Czarnecki, M Mathieu, A Dudzik, J Chung, D H Choi, R Powell, T Ewalds, P Georgiev, et al. Grandmaster level in starcraft ii using multi-agent reinforcement learning. *Nature*, 575(7782):350–354, 2019.

[Watkins and Dayan, 1992] C JCH Watkins and P Dayan. Q-learning. *Machine learning*, 8:279–292, 1992.

[Whitley *et al.*, 1993] D Whitley, S Dominic, R Das, and C W Anderson. Genetic reinforcement learning for neurocontrol problems. *Machine Learning*, 13(2–3):259–284, 1993.

[Williams, 1992] R J Williams. Simple statistical gradient-following algorithms for connectionist reinforcement learning. *Machine learning*, 8:229–256, 1992.

## Supplementary Material

### 1 Setup

For our experiments, we utilized three computing machines. The first machine was configured with an AMD 3950x processor, 16 CPU cores, 64 GB of RAM, and a GeForce RTX 3060 GPU. The second machine contained an Intel Core i9-13900K processor with 24 CPU cores and was equipped with 32 GB of RAM. The third machine was a Debian 12 server running on two AMD EPYC 7662 64-core processors and 1 000 GB RAM. The first two machines were used for obtaining the results for the gradient-based algorithms, the third was used for running the experiments with the ES, which do not require GPU acceleration.

## 2 Additional Results and Hyperparameter Settings

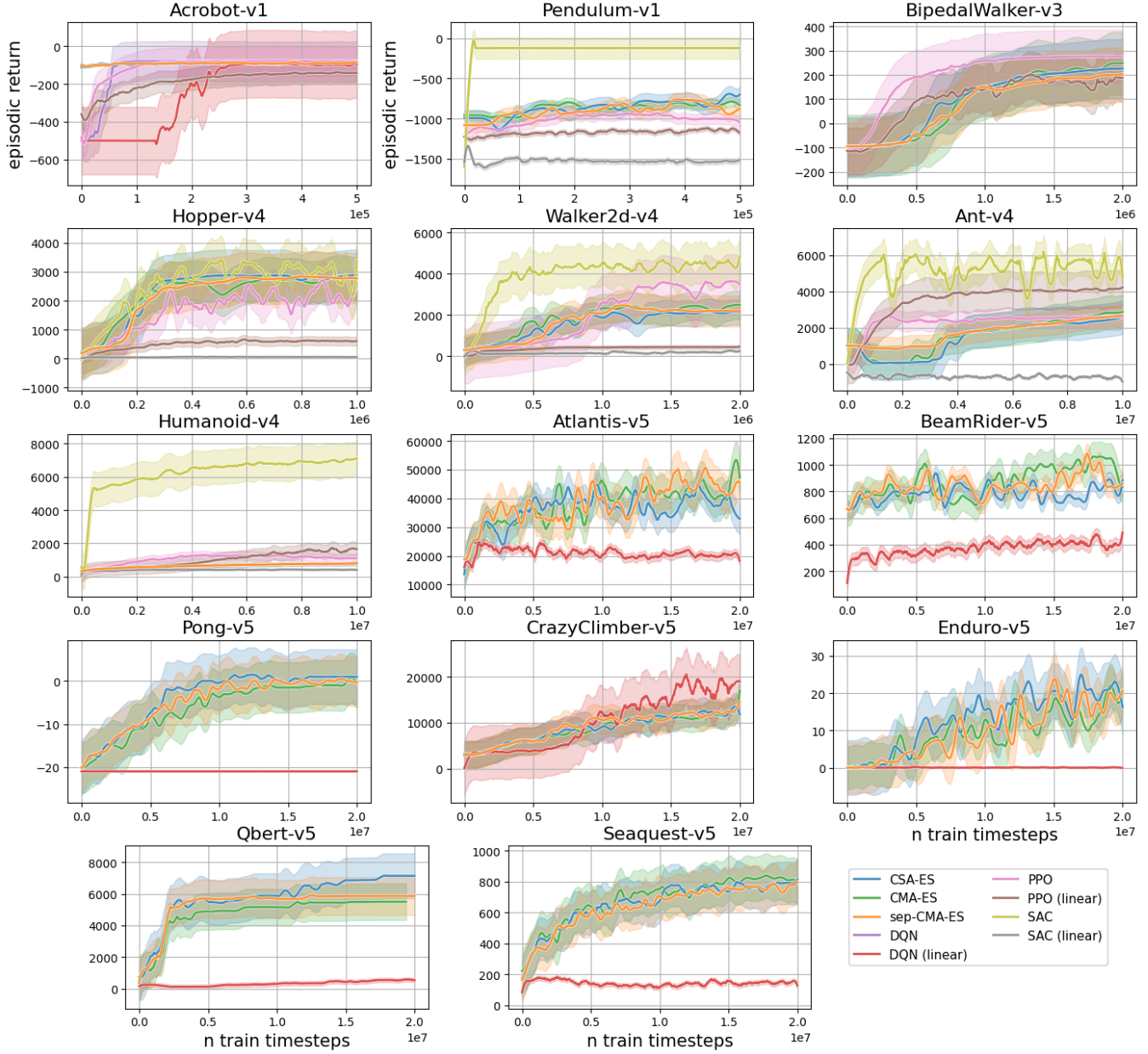


Figure 1: Training curves for the Classic, MuJoCo, and Atari environments. Episodic return (calculated using 5 test episodes) versus the number of training timesteps is shown. Each curve represents the median of 5 trial runs conducted with different random seeds; the shaded area denotes standard deviations. In the classic control environment Acrobot, linear ES solve the environment within few timesteps, exceeding the performance of gradient-based methods. In contrast, classic SAC excels in the Pendulum task and is the only method that achieves the maximum reward of 0. In the BipedalWalker environment, while classic PPO achieves the optimal reward of 300, both linear ES and linear PPO are not far behind in their performance. In the MuJoCo tasks, ES match the performance of the original DRL networks in Hopper, while the linear gradient-based methods struggle to learn a good policy. In Ant, Humanoid, and Walker2d, classic SAC emerges as the dominant method. Linear ES performs comparably to classic PPO, while linear PPO and linear SAC have difficulty finding a good policy. Interestingly, in the Ant environment, linear PPO succeeds in identifying an effective policy and even surpasses the performance of the larger PPO network. In the Atari environments Atlantis, BeamRider, Pong, Crazy Climber, Enduro, Qbert, and Seaquest, linear ES learns effective policies from the game's RAM as policy input. However, linear DQN fails to do the same, except for CrazyClimber and surpasses ES in performance.

Algorithm	CSA-ES	CMA-ES	sep-CMA	Random	Human	DQN	ES*
	M(SD)	M(SD)	M(SD)			M(SD)	
Atlantis	84690 (1.3·10 <sup>4</sup> )	87100 (1.1·10 <sup>4</sup> )	<b>88580</b> (9.1·10 <sup>3</sup> )	12850	29028	85641 (1.7·10 <sup>4</sup> )	103500
B. Rider	2215 (1088)	1967 (582)	2222 (721)	363.9	5775	<b>6846</b> (1619)	5072
Boxing	96.0 (3.8)	<b>96.8</b> (3.2)	95.1 (4.3)	0.1	4.3	71.8 (8.4)	100
C. Climber	36170 (1.0·10 <sup>4</sup> )	29290 (6.5·10 <sup>3</sup> )	32940 (7.8·10 <sup>3</sup> )	10781	35411	<b>114103</b> (2.2·10 <sup>4</sup> )	57600
Enduro	65.1 (22.1)	58.9 (17.8)	69.0 (22.9)	0	309.6	<b>301.8</b> (24.6)	102
Pong	5.7 (4.0)	7.4 (10.3)	7.1 (9.4)	-20.7	9.3	<b>18.9</b> (1.3)	21
Q*Bert	7355 (4037)	5732 (2339)	7385 (3384)	163.9	13455	<b>10596</b> (3294)	14700
Seaquest	959 (204)	948 (117)	954 (143)	68.4	20182	5286 (1310)	1470
S. Invaders	1640 (567)	1972 (332)	1488 (191)	148	1652	<b>1976</b> (893)	2635

Table 1: Average maximum score per game across trials. The rightmost column shows the best-performing ES episode per game. For comparison, the scores for DQN, a random agent, and a Human player taken from [Mnih *et al.*, 2015] are shown. The highest average scores are shown in boldface. The results show that ES achieve the highest scores in two games: sep-CMA attain the highest score in Atlantis and CMA-ES in Boxing, outperforming the Human player and DQN. For the other games, the highest score is attained by the DQN agent, although CMA-ES achieves a score almost identical to DQN on SpaceInvaders. Furthermore, the best ES policy often matches the performance of DQN, demonstrating that a linear policy can be equally effective.

Environment	Inputs	Outputs	Weights
CartPole-v1	4	2	8
Acrobot-v1	6	3	18
Pendulum-v1	3	1	3
LunarLander-v2	8	4	32
BipedalWalker-v3	24	4	96
Swimmer-v4	8	2	16
Hopper-v4	11	3	33
HalfCheetah-v4	17	6	102
Walker2d-v4	17	6	102
Ant-v4	27	8	216
Humanoid-v4	376	17	6392
Atari	128	[4, 18]	[512, 2304]

Table 2: Overview of the dimensionality of states and actions and the corresponding number of trainable weights for the linear neural network architecture.

	$\sigma^{(0)}$	$\lambda$
CartPole	0.1	4
Acrobot	0.05	4
Pendulum	0.1	$\lambda_{\text{DEF}}$
LunarLander	0.1	$\lambda_{\text{DEF}}$
BipedalWalker	0.1	$\lambda_{\text{DEF}}$
Swimmer	0.1	4
HalfCheetah	0.05	$\lambda_{\text{CMA}}$
Hopper	0.05	$\lambda_{\text{DEF}}$
Walker2d	0.05	$\lambda_{\text{DEF}}$
Ant	0.05	$\lambda_{\text{DEF}}$
Humanoid	0.01	$\lambda_{\text{DEF}}$
Atari	1.0	$\lambda_{\text{DEF}}$

Table 3: Hyperparameters used in the ES configuration  $\lambda_{\text{DEF}} = \min(128, \max(32, \frac{n}{2}))$ ,  $\lambda_{\text{CMA}}$ : see [Hansen and Ostermeier, 2001].

	Timesteps	CSA-ES	CMA-ES	sep-CMA-ES	DQN	PPO	SAC	DQN*	PPO*	SAC*
CartPole-v1	$5 \cdot 10^5$	500	500	500	500	500	-	17	197	-
Acrobot-v1	$5 \cdot 10^5$	-75	-73	-75	-65	-69	-	-76	-133	-
Pendulum-v1	$5 \cdot 10^5$	-669	-668	-731	-	-805	-125	-	-955	-1063
LunarLander-v2	$5 \cdot 10^5$	268	273	269	242	145	-	-18	-37	-
BipedalWalker-v3	$2 \cdot 10^6$	228	237	190	-	278	-	-	214	-
Swimmer-v4	$5 \cdot 10^5$	281	315	273	-	62	50	-	33	30
HalfCheetah-v4	$3 \cdot 10^6$	4873	4705	4623	-	2566	14662	-	2254	150
Hopper-v4	$1 \cdot 10^6$	2594	2913	2721	-	2938	3620	-	910	138
Walker2d-v4	$2 \cdot 10^6$	1924	2359	2545	-	4003	3790	-	490	766
Ant-v4	$1 \cdot 10^7$	2647	2819	2684	-	2904	6372	-	4467	-28
Humanoid-v4	$1 \cdot 10^7$	821	-	830	-	2490	7282	-	3561	652

Table 4: Maximum episodic return for each environment averaged over five trials; each trial uses the number of training timesteps specified in the table. Linear networks are marked with a \* symbol. The table shows that ES and DRL vary in effectiveness across tasks. For example, in simpler tasks like CartPole, ES all achieve a maximum score of 500, matching the performance of classic DQN and classic PPO. However, in the more complex MuJoCo tasks, classic gradient-based methods, particularly SAC, outperform ES. Despite this, linear ES algorithms consistently outperform their linear gradient-based counterparts across various environments, suggesting that gradient-based algorithms may be less effective at discovering linear strategies than ES algorithms.

	Threshold	CSA-ES	CMA-ES	sep-CMA-ES	DQN	PPO	SAC	DQN*	PPO*	SAC*
CartPole-v1	475	$3 \cdot 10^3$	$2 \cdot 10^3$	$3 \cdot 10^3$	$2 \cdot 10^4$	$6 \cdot 10^4$	-	$\infty$	$\infty$	-
Acrobot-v1	-100	$4 \cdot 10^3$	$5 \cdot 10^3$	$4 \cdot 10^3$	$2 \cdot 10^4$	$7 \cdot 10^4$	-	$1 \cdot 10^5$	$\infty$	-
Pendulum-v1	-100	$\infty$	$\infty$	$\infty$	-	$\infty$	$\infty$	-	$\infty$	$\infty$
LunarLander-v2	200	$5 \cdot 10^4$	$7 \cdot 10^4$	$6 \cdot 10^4$	$3 \cdot 10^5$	$4 \cdot 10^5$	-	$\infty$	$\infty$	-
BipedalWalker-v3	300	$2 \cdot 10^6$	$2 \cdot 10^6$	$5 \cdot 10^6$	-	$\infty$	-	-	$\infty$	-
Swimmer-v4	360	$4 \cdot 10^5$	$3 \cdot 10^5$	$7 \cdot 10^5$	-	$\infty$	$\infty$	-	$\infty$	$\infty$
HalfCheetah-v4	4800	$2 \cdot 10^6$	$1 \cdot 10^6$	$2 \cdot 10^6$	-	$\infty$	$5 \cdot 10^4$	-	$\infty$	$\infty$
Hopper-v4	3000	$4 \cdot 10^5$	$3 \cdot 10^5$	$1 \cdot 10^6$	-	$3 \cdot 10^5$	$1 \cdot 10^5$	-	$\infty$	$\infty$
Walker2d-v4	3000	$6 \cdot 10^6$	$9 \cdot 10^5$	$1 \cdot 10^6$	-	$7 \cdot 10^5$	$1 \cdot 10^5$	-	$\infty$	$\infty$
Ant-v4	5000	$3 \cdot 10^7$	$3 \cdot 10^7$	$2 \cdot 10^7$	-	$\infty$	$4 \cdot 10^5$	-	$\infty$	$\infty$
Humanoid-v4	6000	$\infty$	-	$5 \cdot 10^7$	-	$\infty$	$1 \cdot 10^6$	-	$\infty$	$\infty$

Table 5: Lowest number of timesteps required to reach threshold reward, in any of the five trial runs. The  $\infty$  symbol indicates that the threshold was not attained, and the '-' symbol indicates no available data. In less complex tasks such as CartPole and Acrobot, ES consistently attain the threshold reward more quickly than DRL, requiring only a few thousand timesteps compared to the tens of thousands needed by gradient-based methods. In more complex tasks like HalfCheetah and Ant, DRL methods, especially SAC, tend to reach the threshold more efficiently, with SAC achieving it in just 50.000 timesteps for HalfCheetah and 400.000 for Ant, compared to millions of timesteps needed by ES algorithms. It is important to note that although ES require more timesteps than DRL methods, this doesn't necessarily translate to longer wallclock time, as ES can be effectively parallelized. In the Swimmer task, ES achieve the threshold in 300.000 to 700.000 timesteps, while DRL methods fail to reach the threshold.

Layer	Number of Nodes
Input Layer	Size of observation space
ReLU Hidden Layer 1	120
ReLU Hidden Layer 2	84
Output Layer	Size of action space

Table 6: DQN architecture. In contrast to the original DQN, which utilizes convolutional layers for image processing, our approach is tailored for non-image data. This configuration is adapted from the CleanRL implementation, which has been tested and performed well on several control tasks [Huang *et al.*, 2022].

Parameter	Value
Optimizer	Adam
Learning rate	$2.5 \cdot 10^{-4}$
Discount factor ( $\gamma$ )	0.99
Replay buffer size	$1 \cdot 10^4$
Target network update frequency (timesteps)	500
Batch size	128
Start- $\epsilon$	1
End- $\epsilon$	0.05
Fraction of timesteps to go from start- $\epsilon$ to end- $\epsilon$	0.5

Table 7: DQN hyperparameters. This configuration is adapted from the CleanRL implementation, which has been tested and performed well on several control tasks [Huang *et al.*, 2022].

Component	Layer	Number of Nodes
Critic	Input Layer	Observation space size
	Tanh Hidden Layer 1	64
	Tanh Hidden Layer 2	64
	Output Layer	1
Actor	Input Layer	Observation space size
	Tanh Hidden Layer 1	64
	Tanh Hidden Layer 2	64
	Output Layer	Action space size

Table 8: PPO architecture. The PPO architecture employs the same actor-critic network structure as introduced in the original paper [Schulman *et al.*, 2017]

Hyperparameter	Value
Horizon (T)	128
Optimizer	Adam
Clip coefficient ( $\epsilon$ )	0.2
Discount factor ( $\gamma$ )	0.99
GAE parameter ( $\lambda$ )	0.95
Mini batch size	32

Table 9: PPO hyperparameters. Hyperparameters used for the Classic Control tasks, based on [Schulman *et al.*, 2017]

Hyperparameter	Value
Horizon (T)	2048
Optimizer	Adam
Clip coefficient ( $\epsilon$ )	0.2
Discount factor ( $\gamma$ )	0.99
GAE parameter ( $\lambda$ )	0.95
Mini batch size	64

Table 10: PPO hyperparameters. Hyperparameters used for the MuJoCo tasks, based on [Schulman *et al.*, 2017]

Component	Layer	Number of Nodes
Actor	Input Layer	Observation space size
	ReLU Hidden Layer 1	256
	ReLU Hidden Layer 2	256
	Output Layer (Mean)	Size of action space
	Output Layer (Log Std)	Size of action space
Critic	Input Layer	Observation space size + Action space size
	ReLU Hidden Layer 1	256
	ReLU Hidden Layer 2	256
	Output Layer	1

Table 11: SAC architecture: SAC employs the same actor-critic network structure as introduced in the original paper [Haarnoja *et al.*, 2018]

Parameter	Value
Optimizer	Adam
Policy learning rate	$3 \times 10^{-4}$
Q network learning rate	$1 \times 10^{-3}$
Discount factor ( $\gamma$ )	0.99
Replay buffer size	$10^6$
Mini batch size	256
Entropy target	- dimension(action space)
Target smoothing coefficient ( $\tau$ )	0.005
Target update interval	1

Table 12: SAC hyperparameters, based on [Haarnoja *et al.*, 2018]